Bioabsorbable Interlocked Nail System For 3D Printed Segmental Bone Defects

By

Hussein Alizereej

Master of Science in Engineering Physics-Mechanical Engineering

University of Central Oklahoma

Edmond, Oklahoma

August 2024

Master Thesis

Thesis submitted to the Faculty of the Graduate College of the University of Central Oklahoma in partial fulfillment of the requirements for the master's degree.

2

Bioabsorbable Interlocked Nail System For 3D Printed Segmental Bone Defects

Thesis approval

Committee Chairperson: Dr. Morshed khnadaker

Committee Member: Dr. Benjamin Tayo

Committee Member: Dr. Abdellah Ait Moussa

Acknowledgment

My sincere appreciation goes out to my supervisor, Dr. Morshed Khandaker, for all his helpful advice, steadfast support, and perceptive criticism during the dissertation process. The direction and caliber of this work have been greatly influenced by their knowledge and support.

Additionally, I owe a debt of gratitude to Abdellah Ait Moussa, Ph.D. and Benjamin Tayo, Ph.D., who served on my thesis committee. Their assistance, knowledge, and helpful critiques significantly improved the thoroughness and depth of my study.

I extend my heartfelt thanks to University of Central Oklahoma for providing the necessary resources and conducive environment for carrying out this study.

I sincerely thank my elder Brother Mr. Ayman Zuhair for his love, compassion, and patience during this difficult time. This achievement would not have been possible without him. His constant support was a constant source of inspiration and financial support. He has been a father figure and a great mentor throughout my life. I dedicate this work to him.

Lastly, Also a special thank you for Reuben Lane and Shannon Yeakley for being part of this study . I acknowledge the countless individuals who participated in this study, without whom this research would not have been possible.

Thank you all for being part of this endeavor.

Hussein Alizereej

Table of Contents

List of Figures and tables

Figure 28. a) The 3D printed targeting jig. (b) Efficacy tests of the fabricated delivery jigs using a 3D-printed rabbit tibia model, demonstrating the jig's capability to install an intramedullary nail and screws into a 20 mm-long rabbit tibia defect

Figure 29. First leg: (a) Creation of a 20 mm long bone defect using an orthopedic oscillating bone saw; (b) Formation of intramedullary holes for the nail; (c) Scaffold installation with interlocking nails; and (d) Secure fastening of nails to the tibia bone using a screw. Second leg: (e) Secure fastening of the scaffold with a nail through a screw in an installed interlocking nail system within a long bone defect model.

Table 1. Comparative Analysis of Interlocking Nail System Materials

Abstract

Advancements in three-dimensional (3D) printing and biomaterials have revolutionized bioengineering, particularly in medical applications. This study aims to develop cost-effective bioabsorbable scaffolds and interlocked nails for bone repair, focusing on segmental bone defects, which can cause significant functional impairments and cosmetic deformities. The research utilizes a rabbit tibia model to test the efficacy of these innovations. Bioabsorbable scaffolds and interlocked nails show promise in enhancing bone repair outcomes and minimizing the need for additional surgeries. Using 3D printing to fabricate these systems has proven more effective than traditional methods. The study employs biocompatible and biodegradable materials, specifically polycaprolactone (PCL) and PCL combined with MgO, to create the scaffold, interlocking nail, and screws through a phase separation casting method. This technique allows precise control over the scaffold's pore structure and size and facilitates the incorporation of bioactive agents or cells into the scaffold matrix. In the first phase of the study, the PCL scaffolds demonstrated suitability for accelerated degradation and early weight-bearing capacity. The second phase focused on the accurate placement of the scaffold and fixation system using the rabbit tibia model. A surgical jig was designed and fabricated from biocompatible resin, with a 3D model printed using computer-aided design (CAD) software. Stereolithography (SLA) 3D printing technology was employed in the photopolymerization process, followed by UV light curing to enhance the jig's strength.Experiments on cadaver models using New Zealand white rabbits confirmed that the scaffold, intramedullary nail, and screw system are strong enough to support load-bearing areas of surgical insertions. The designed prototype shows potential for

further clinical translational studies, demonstrating the effectiveness and practical application of the scaffold and fixation system in reconstructive surgeries for long-bone segmental defects.

Chapter 1

Introduction

1.1 Background

Segmental or long bone defect is a condition where a void or cavity in the bone fails to heal naturally, often caused by trauma, tumor, or infection.(Mauffrey et al.) Orthopedic surgeons face significant challenges in treating these defects due to limitations in using the patient's bone for grafting. In response, a project was initiated to develop a solution: a 3D-printed scaffold implant designed to enhance cell growth within these bone defects. Additionally, an interlocking nail system was created to secure the scaffold in place.(Khandaker et al.)

This interlocking nail system, consisting of an intramedullary nail and trans-fixation screws, has proven effective in repairing long bone defects in various animal models. Adapting this system for repairing a rabbit's tibia, which is smaller than previous applications, was the focus of this project. Alongside the interlocking nail system, the scaffold implant was employed to fill the void left by the bone defect. (Khandaker et al.) Together, these technologies aim to stimulate tissue growth across critical-size long bone defects while offering mechanical support for weight-bearing activities. (Khandaker et al.)

The scaffold material was crafted from polycaprolactone (PCL), while the nail system utilized a composite of PCL and magnesium (PCL-Mg). The final products included the scaffold implant, intramedullary nail and screws (interlocking nail system), and a targeting jig. (Khandaker et al.)

Additionally, alternative treatment methods for segmental bone defects include distraction osteogenesis, induced membrane techniques, vascularized fibular transplantation, and the gradual shortening of the limb using halo-type equipment to facilitate natural healing. (Yang et al.; Khandaker et al.)

In conclusion, the project sought to tackle the challenges associated with segmental bone defects by combining 3D printed scaffold technology with an interlocking nail system; to promote tissue growth and provide mechanical support for effective bone repair.

1.2 Current Solutions

Current surgical approaches for treating segmental defects in long bones are characterized by their invasiveness, requiring multiple surgeries and prolonged recovery periods, often hindering the ability to bear weight. (Ferreira and Tanwar) Commonly utilized treatment methods include distraction osteogenesis, induced membrane techniques, and vascularized fibular transplantation, each with distinct advantages, drawbacks, and associated risks.(Yang et al.; Khandaker et al.) Another approach involves the gradual shortening of the limb using halo-type equipment, facilitating natural repair by bringing the ends of the bone defect closer together. However, this method often results in permanent limb shortening.

Despite the availability of these treatments, scaffold implants are not currently utilized in human segmental bone defect repair. Nevertheless, ongoing research utilizing various animal models aims to assess their effectiveness. Polymeric materials, such as Polycaprolactone (PCL), offer precise control over scaffold properties such as pore size, porosity, solubility, biocompatibility, enzymatic responses, and allergic reactions.(Coombes et al.)

Various methods are employed to address segmental bone defects, typically involving invasive procedures, multiple surgeries, protracted recovery times, and limited weight-bearing capabilities. One such technique entails the insertion of an intramedullary nail into the bone cavity, secured with screws passing through the bone and nail. However, the lack of a commercially available interlocking mechanism designed specifically for rabbits' results in some instability with these nails. Additionally, prior studies using rabbit models have utilized stainless steel for intramedullary nails, necessitating an additional surgery for removal, which is suboptimal for human implants.

1.3 Impact statement

At present, standardized treatment methods for critical-size long-bone segmental defects in humans are lacking, with current solutions proving unsatisfactory, necessitating multiple complex surgeries, posing a high risk of infection, and often resulting in lifelong difficulties for patients. (Khandaker et al.) There is an urgent need for a novel solution that not only fosters bone union and allows weight bearing during the healing process but also requires minimally invasive surgeries. (Khandaker et al.)The ongoing study marks the initial step towards potential future human applications. Key aspects of the proposed solution include the reduced size of the intramedullary nail and fixation screws, as well as the bioabsorbable nature of the scaffold and fixation system. (Khandaker et al.)This unique combination of an intramedullary nail and scaffold fixation enables early load-bearing post-surgery while eliminating the need for subsequent surgeries typically associated with non-bioabsorbable implants. Furthermore, it facilitates the gradual filling of the space left by the implants as they dissolve over time. (Khandaker et al.)

Moreover, there is currently no commercially available interlocking mechanism designed specifically for rabbits, resulting in some degree of instability with these nails. Additionally, previous studies utilizing rabbit models have employed stainless steel for intramedullary nails, which may not be optimal for human implants and necessitates additional surgery for nail removal.

1.4 Proposed Solution

Our strategy for addressing segmental bone defects involves employing a rabbit tibia model and integrating a bioabsorbable interlocking nail system along with a scaffold implant for the bone void. Our approach presents several enhancements compared to current methods:

1. Improved stability achieved through the utilization of an interlocking nail system.
2. Immediate post-surgery load-bearing capacity facilitated by the nail and scaffold implant.
3. Promotion of bone union without causing leg shortening, facilitated by the scaffold.
4. Elimination of the necessity for additional surgeries to remove implants due to their bioabsorbable nature.
5. Facilitation of bone cell migration to occupy the void left by the implants as they gradually dissolve over time. (Khandaker et al.)

The uniqueness of our solution lies in the reduced size of the intramedullary nail and fixation screws, along with the bioabsorbable characteristics of the scaffold and fixation system. (Khandaker et al.)This combination enables early post-surgery load bearing and eradicates the need for subsequent surgeries typically associated with non-bioabsorbable implants.

Additionally, it supports gradual bone cell migration into the implant void as the materials degrade over time.

To evaluate the biocompatibility of the bone scaffold and intramedullary nail materials, we conducted a cell viability test using a 48-well plate. The scaffolds, fabricated using various 3D printing techniques, were composed of a polycaprolactone (PCL)-based material. Various tests, including cell viability assays and mechanical tests, were carried out on the scaffold types to assess their material properties.

1.5 Research phases

The initial phase of the research focuses on developing and producing a scaffold and fixation system customized for the reconstruction of long-bone segmental defects in the rabbit tibia model.(Wong et al.) Biocompatible and biodegradable materials, specifically polycaprolactone (PCL) and PCL combined with sodium alginate (PCL-Alg), are employed in the manufacturing process.(Vacanti; Khandaker et al.) The phase separation casting method, a technique for fabricating porous scaffolds in tissue engineering applications tissue scaffolding (Khandaker M), is utilized, offering advantages such as controlled pore structure, size, and the incorporation of bioactive agents or cells.(Fuchs et al.; Grandi et al.; Murry and Keller)

Degradation and mechanical assessments confirm the suitability of PCL and PCL-Alg scaffolds for accelerated degradation and early weight-bearing capacity. (Grandi et al.)The porous surface of the PCL scaffold facilitates the infiltration of alginate hydrogel throughout, contributing to cell viability as indicated by increased cell numbers.(Sudhakar et al.; Grandi et al.)

The subsequent phase focuses on the precise placement of the scaffold and fixation system within the rabbit tibia model. A surgical jig, designed with biocompatible resin and manufactured using Stereolithography (SLA) 3D printing technology, aids in accurate placement.(Wei et al.; Vacanti) The efficacy of the bone scaffolds and interlocking nail and screw system, supported by the novel jigs, is examined through experiments on cadavers using New Zealand white rabbits.(Endo et al.) The results affirm the accurate placement and strength of the system in load-bearing areas.

This study, distinguished in its approach, addresses critical-size long-bone segmental defects. Current solutions are often unsatisfactory, necessitating multiple complex surgeries and carrying a high risk of infection. (Khandaker et al.) The proposed solution, characterized by a reduced intramedullary nail size and bioabsorbable components, offers a promising alternative. This innovation allows for early weight-bearing post-surgery and eliminates the need for follow-up surgeries, fostering gradual bone regeneration.

In summary, this study represents a significant step toward potential future human applications, combining PCL-based scaffolds and a highly biodegradable hydrogel for critical-size bone defects.(Sudhakar et al.) The results provide evidence of the biological activity and cytocompatibility of PCL-based bone substitutes in vitro. Furthermore, the study evaluates the effectiveness of bone substitutes and nail implanting mechanisms using a unique targeting jig on a rabbit tibia model through a cadaveric study. (Khandaker et al.)

1.6. Objective

The amalgamation of advancements in three-dimensional (3D) printing and biomaterials has propelled bioengineering into uncharted territories, particularly within medical applications. This evolution has paved the way for groundbreaking concepts in tissue engineering, giving rise to the development of bioabsorbable scaffolds and interlocked nails designed specifically for bone repair.(Fuchs et al.) This study, centered on addressing prevalent clinical challenges, explores tissue-engineering applications for segmental bone defects, which are common issues leading to functional impairment and cosmetic deformities.

The primary objective of this research is to craft a cost-effective scaffold and fixation system tailored for the reconstruction of long-bone segmental defects in a rabbit tibia model. (Fernandes et al.) The utilization of bioabsorbable scaffolds and interlocked nails holds immense potential to significantly enhance bone repair outcomes, thereby reducing the need for additional surgeries. The integration of 3D printing in the fabrication of these components further contributes to superior outcomes compared to traditional fabrication methods.

Within the study, rabbit tibia models serve as the testing ground for the scaffold and fixation system's intervention in reconstructing long bone segmental defects. (Khandaker et al.)The overarching aim is to assess the effectiveness of biocompatible and biodegradable materials in bone defect reconstruction.(Vacanti) Notably, the scaffolds employed in this study predominantly incorporate pristine cell-based prototypes.

Chapter 2

Materials and Methods

Summary:

This study culminated in the development of the scaffold implant, the interlocking nail system (comprising nails and screws), and a targeting jig. PCL pellets and tetrahydrofuran (THF) solution were employed to fabricate the PCL-based scaffold, interlocking nails, and screws. The scaffold is composed of polycaprolactone (PCL) pellets, with an average size of around 3 mm and a molecular weight of 80,000, making it an FDA-approved biomaterial. (Grandi et al.; Khandaker et al.) Similarly, the nails and screws were fashioned using PCL. Additionally, sodium alginate, calcium chloride, and phosphate-buffered saline (PBS) were utilized in the preparation of the sodium alginate hydrogel. All chemicals were sourced from Sigma-Aldrich (Sigma-Aldrich Co., LLC., St. Louis, MO, USA. (Khandaker et al.)

To create the PCL sodium Alginate solution, sodium alginate powder was mixed with PBS at a ratio of 1 g of sodium alginate per 40 mL of PBS. (Grandi et al.; Khandaker et al.) The mixture was then placed in a beaker on a magnetic stirrer (Corning PC-620D) (Wong et al.), Corning Inc., Corning, New York, NY, USA) set to 150 rpm and 90°C for 2 hours. Once the gel formed, the beaker was covered with parafilm and left to incubate until ready for use. Subsequently, PCL-Alg scaffolds were prepared by immersing the scaffolds in the gel for 5 minutes and then submerging them in a calcium chloride solution. This process promoted cross-linking between calcium ions and alginate polymers, leading to the gel's transformation into a semi-solid state. (Khandaker et al.)

2.1Materials

2.1.1 Hydrogel

A hydrogel, formed by combining a polymer with a liquid that solidifies into a gel while retaining substantial water content, plays a crucial role in filling the voids within the scaffold, emulating the body's extracellular matrix conducive to cell attachment. (Capacchione et al.) Designed with intentional porosity, the scaffold requires the presence of hydrogel to occupy these porous spaces. Illustrated in Figure 1 is a cross-section displaying a porous scaffold devoid of hydrogel at the top and one filled with hydrogel at the bottom, indicated by the tan color.

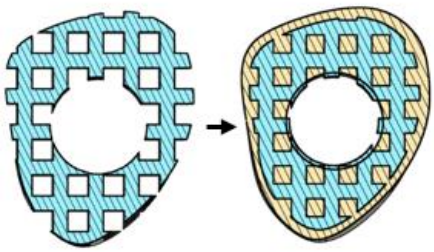

Figure 1. Cross-sectional view comparing a scaffold without hydrogel (left) to one with hydrogel (right).

To produce the sodium alginate hydrogel, sodium alginate powder was blended with phosphate buffered saline (PBS) at a ratio of 1g of sodium alginate per 40mL of PBS. The mixture underwent stirring in a beaker placed on a Corning PC-620D magnetic stirrer (see Figure 2), set to operate at 150 RPM and 90°C for 2 hours. Once the gel formed, the beaker was sealed with parafilm and left to incubate until ready for use. (Khandaker et al.) The preparation of extrusion-based 3D printed scaffolds for testing entailed coating the scaffolds in the gel and

immersing them in a calcium chloride solution. This process facilitated cross-linking between calcium ions and alginate polymers, transforming the gel into a semi-solid state.

Previous research has investigated cell growth on 3D-printed polycaprolactone scaffolds, yielding unsatisfactory outcomes due to excessive gaps between scaffold layers, causing cells to sink and adhere to the bottom. Subsequent experiments involved scaffolds treated or covered with hydrogel, resulting in significantly improved results. The hydrogel functions as an extracellular matrix crucial for cell attachment and offers an optimal environment for cell growth due to its composition.

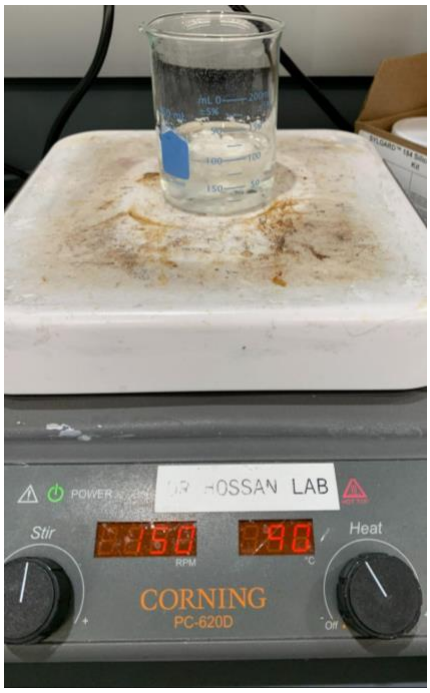

Figure 2. Sodium Alginate gel is being stirred on a hot plate.

2.1.2 Bone scaffold

This study focused on enhancing PCL-based scaffolds to produce osteoconductive bone substitutes in combination with a highly biodegradable hydrogel for critical-size bone defects.(Wong et al.) The research aimed to provide proof of principle and pre-clinical efficacy regarding the biological activity and cytocompatibility of these PCL-based bone substitutes through in vitro experiments. Additionally, the study evaluated the effectiveness of bone substitute and nail implanting mechanisms on a rabbit tibia model using a unique targeting jig, as assessed through cadaveric studies.

In the context of bone defect treatment, current options typically do not involve the use of a bone scaffold implant. However, alternative approaches, such as distraction osteogenesis, induced membrane, and vascularized fibular transplantation, are being explored with various animal models.(Yang et al.) While each of these options has its advantages, they also come with significant drawbacks and complications.(Yang et al.) Another treatment option involves the use of a halo-type apparatus to gradually shorten the limb, allowing the body to repair the defect naturally, albeit resulting in a permanently shorter limb. Overall, scaffold implants are not currently employed in human segmental bone defect repair. Polymeric materials, like Polycaprolactone (PCL), offer more control over the physicochemical properties of scaffolds, including pore size, porosity, solubility, biocompatibility, enzymatic responses, and allergic reaction.(Grandi et al.)

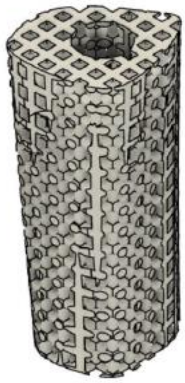

Figure 3**.** Polymer scaffold

Polycaprolactone (PCL) is widely employed in tissue engineering and drug delivery due to its versatile properties. Utilizing micro-computed tomography, researchers can create detailed three-dimensional (3D) models of long bone scaffolds and interlocking nails in rabbits.(Fuchs et al.; Wei et al.) PCL-based scaffolds have been effectively used as substitutes for bone fractures. However, there is a noticeable gap in research concerning the utilization of PCL-based scaffold and fixation systems for addressing segmental bone defects in rabbit tibias. While current treatment options for such defects typically do not involve scaffold implants, ongoing studies are investigating their potential efficacy with various animal models. Alternative treatment methods for segmental bone defects, such as distraction osteogenesis, induced membrane techniques, and vascularized fibular transplantation, offer benefits but are accompanied by significant drawbacks and complications.(Yang et al.) Another approach entails the use of halo-type equipment to gradually shorten the limb, facilitating the natural repair of bone defects. Nevertheless, this

method results in permanent limb shortening. At present, scaffold implants are not commonly employed in the repair of human segmental bone defects.

2.1.2.1 PCL

All scaffolds utilized in this study are based on polycaprolactone (PCL). The PCL nanofiber cloths underwent treatment with sodium alginate hydrogel to enhance their biomedical performance.

The preparation of PCL scaffolds in this study employed the Phase Separation Casting Method. crafting in vitro samples, a 10-mm diameter and 5-mm height silicone mold were utilized, while for ex vivo samples, a 20-mm scaffold modeled after a rabbit tibia was created. A resin (SLA) printing technique was applied, selecting resin-printed masterpieces made of photopolymer resin for their precision in generating negative molds for two-part silicone molds. (Khandaker et al.)

2.1.2.2 PCL-Sodium Alginate

To create a sodium alginate (Alg) hydrogel solution for coating a PCL scaffold, a ratio of 1 g of sodium alginate powder to 40 mL of phosphate-buffered saline (PBS) was employed. These components were combined in a beaker and positioned on a magnetic stirrer (Corning PC-620D, Corning Inc., Corning, New York, NY, USA).(Dang et al.; Khandaker et al.) A magnetic stir bar was inserted into the beaker, and the hot plate stirrer settings were adjusted to 150 rpm and 90 °C for a duration of 2 hours. (Dang et al.)After the gel formation, the beaker was sealed with parafilm and incubated until ready for use.

To the preparation of PCL-Alg scaffolds, the scaffolds were immersed in the gel for 5 minutes and subsequently submerged in a calcium chloride solution. (Khandaker et al.)This crucial step

facilitates cross-linking between calcium ions and alginate polymers, transforming the gel into a semi-solid state.

Polymeric materials like PCL provide precise control over scaffold physicochemical properties, including pore size, porosity, solubility, biocompatibility, enzymatic responses, and allergic reactions. Various scaffold designs, such as extrusion-based 3D printing, electro-spun Nanofiber methods, and casting methods, all utilize PCL as a base material.

2.2 Methods

2.2.1 Extrusion-Based 3D Printing Method

Initially, the extrusion-based 3D printing method was employed to create the scaffold using an ESP printer as shown in Figure 4. This printer utilizes a PCL filament and operates by following programmed codes to control the x, y, and z axes. The process is relatively straightforward: the three-axis controller orchestrates the movement, while a 0.2 mm diameter nozzle on the z-axis deposits the filament, forming the scaffolds. Essentially, its operation mirrors that of a standard 3D printer. The final step involves directing cold air from a fan onto the scaffold, cooling and solidifying the filament to maintain its shape. To ensure accuracy, a custom-made 3D printer with high precision was utilized, capable of producing scaffolds shown in Figure 5 measuring 3mm, 5mm, and 10mm. However, the machine's constraints restricted the fabrication of scaffolds exceeding 10mm in length.

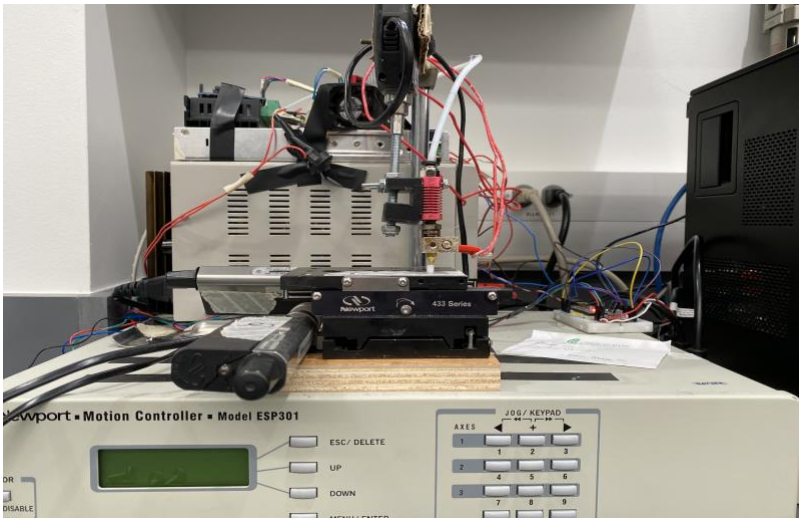

Figure 4. ESP Printer

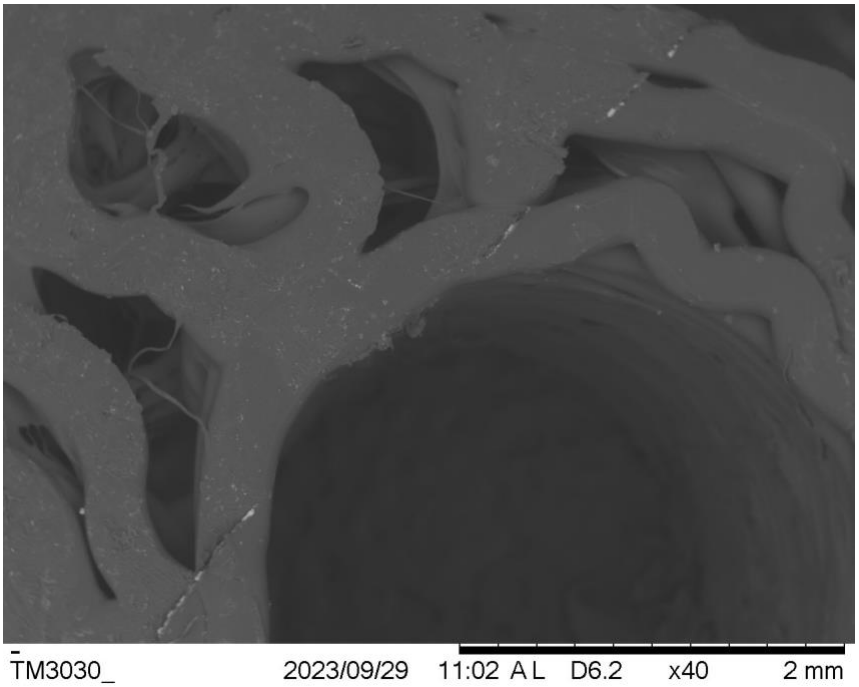

Figure 5. Bone Scaffolds MSE image

2.2.2 Electro-Spun Nanofiber Method

We employed another method involving the fabrication of scaffolds from layers of electro-spun nanofiber. The process commenced by generating nanofiber material using an electrospinning nanofiber machine located in the nanobiology lab, illustrated in Figure 6. To prepare PCL for this method, 0.5g of PCL pellets were mixed with 5g of acetone and subjected to sonication for 30 minutes. (Khandaker et al.)The resulting mixture was then loaded into a syringe equipped with a needle and placed onto the machine, as seen in Figure 6. One end of the needle was connected to a positive lead, while the spinning rod was attached to the negative lead. Activating the machine applied high voltage, generating a magnetic field that charged the PCL, causing it to be attracted to the spinning rod. As the rod rotated, layers of PCL nanofibers accumulated, gradually building up the thickness of the cloth. Periodic lateral movement of the rod ensured uniform thickness throughout the cloth. Once the desired size of the nanofiber cloth was attained, the machine was deactivated, and a blade was used to remove the cloth from the rod, resulting in a rectangular sheet of electro-spun nanofiber.

- The nanofiber cloth illustrated in Figure 7 was created using the electrospinning technique.
- Three materials were tested:

1.PCL

2. PCL + Magnesium

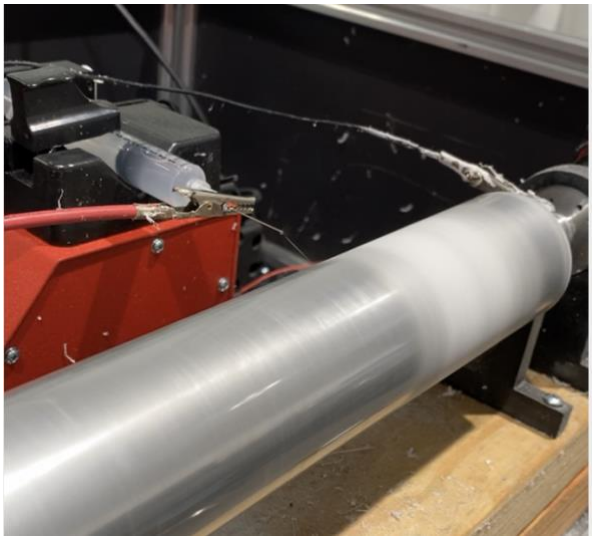

Figure 6. Electrospinning Nanofiber Machine

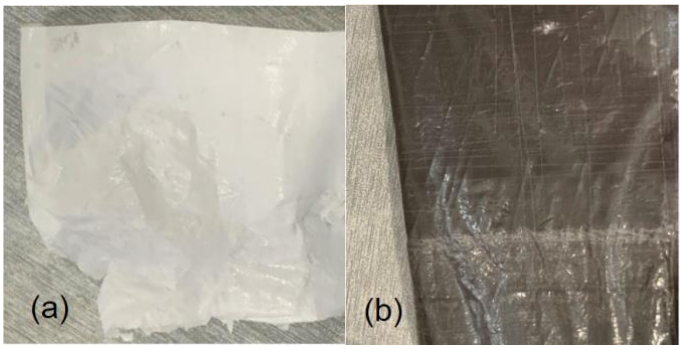

Figure 7. (a) Nanofiber cloth (b) PCL-Mg nanofiber.

PCL nanofiber cloths were enhanced with sodium alginate hydrogel to enhance their biomedical performance. Subsequently, the nanofiber cloth can be soaked with alginate to prepare PCL-sodium alginate cloth and cured with calcium chloride to PCL-Alg 3D scaffold as shown in Figure 8.

Figure 8. Nanofiber Cloth wrapped around Nail.

2.2.3 Phase Separation Casting Method

The third method attempted to fabricate a scaffold involved casting. Initially, a 20mm scaffold was modeled and resin (SLA) printed. This printed scaffold was then cured with UV light for 2 hours to remove excess sulfur and brushed with an acrylic coating. Two-part silicone molds, incorporating embedded rods to ensure a hollow center, were created using the resin scaffold as a master.

Z the casting process, a phase separation technique detailed in studies by Grandi et al. (Grandi et al.) and Coombes et al. (Coombes et al.)was employed. PCL pellets were dissolved in 10ml of tetrahydrofuran (THF) at a ratio of 17.5% wt/wt. through constant agitation in an orbital shaker until a uniform solution was achieved. Distilled water equivalent to 50% of the solution's weight was then added while stirring until two phases formed: an aqueous phase and a gel phase. The aqueous phase was discarded, and the gel phase was transferred to a syringe and injected into a pre-cooled silicone mold (-20°C). The mold was left to cure at -20°C overnight. After curing, the

scaffold was removed from the mold, washed in ethanol to remove the solvent, and allowed to dry at room temperature, resulting in a microporous PCL scaffold.

In addition to a pure PCL scaffold, a PCL-hydroxyapatite (PCL-HA) scaffold was produced by incorporating an amount of HA powder equal to the weight of PCL in the initial THF solution, based on the study by Coombes et al. (Coombes et al.) The mold used for in vitro samples was a 10-mm diameter and 5-mm height silicone mold available in the laboratory. For ex vivo samples, a 20-mm scaffold was modeled from a rabbit tibia model, resin (SLA) printed, cured with UV light for 2 hours, and brushed with a lubricant. Two-part silicone molds, also incorporating embedded rods, were created using the resin scaffold as a master. Resin-printed masterpieces were chosen for their precision in creating negative molds, with silicone used to form the two-part mold for casting the scaffolds and securing them in place during curing.

The casting process followed the phase separation technique detailed earlier, resulting in microporous PCL scaffolds. To ensure a hollow center, embedded rods were incorporated into both in vitro and ex vivo molds. The resin scaffold served as the master for creating two-part silicone molds, facilitating the casting of both scaffolds and the nail and screws with the assistance of rubber bands. Additional holes were integrated into the molds to secure rods during the curing process.

All scaffolds utilized in this study are based on polycaprolactone (PCL). The PCL nanofiber cloths underwent treatment with sodium alginate hydrogel to enhance their biomedical performance. The casting process followed the phase separation technique detailed by Grandi et al. and Coombes et al.(Grandi et al.; Coombes et al.), outlined in Figure 10. In summary, PCL pellets were dissolved in 10 mL of tetrahydrofuran (THF) at a 17.5% wt/wt ratio, forming a uniform solution through constant agitation. The addition of distilled water, accounting for 50%

of the solution's weight, induced phase separation, resulting in aqueous and gel phases. The gel phase, containing PCL, was injected into a pre-cooled silicone mold, and left to cure at -20 °C overnight. Following curing, the scaffold underwent ethanol washing to remove the solvent, dried at room temperature and produced a microporous PCL scaffold. This phase separation casting technique provides precise control over physicochemical properties, yielding well-defined scaffolds suitable for the study's objective.

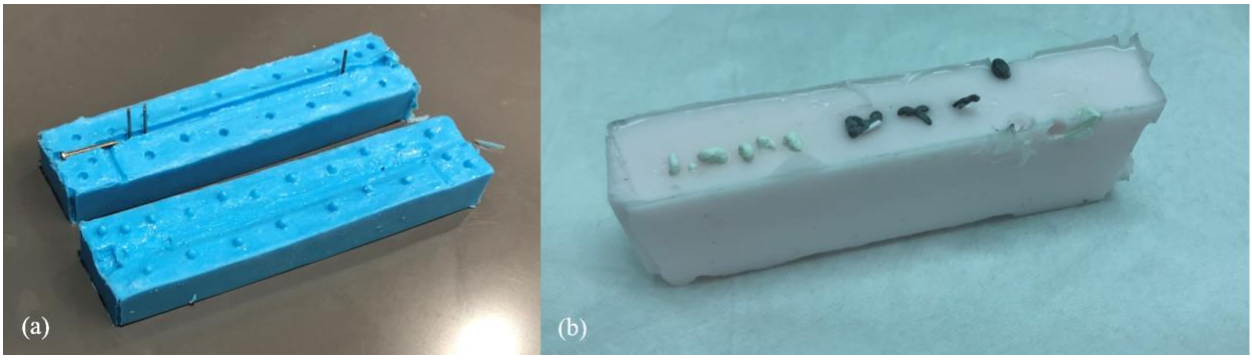

Figure 9. Silicone molds were utilized for creating various components: (a) bone scaffold, (b) interlock nail and screws,

All scaffolds utilized in this study are based on polycaprolactone (PCL). The PCL nanofiber cloths underwent treatment with sodium alginate hydrogel to enhance their biomedical performance.(Grandi et al.) The casting process followed the phase separation technique detailed by Grandi et al. and Coombes et al. (Grandi et al.; Coombes et al.), outlined in Figure 10. In summary, PCL pellets were dissolved in 10 mL of tetrahydrofuran (THF) at a 17.5% wt/wt ratio,

forming a uniform solution through constant agitation. The addition of distilled water, accounting for 50% of the solution's weight, induced phase separation, resulting in aqueous and gel phases. The gel phase, containing PCL, was injected into a pre-cooled silicone mold, and left to cure at -20 °C overnight. Following curing, the scaffold underwent ethanol washing to remove the solvent, dried at room temperature and produced a microporous PCL scaffold. This phase separation casting technique provides precise control over physicochemical properties, yielding well-defined scaffolds suitable for the study's objective.

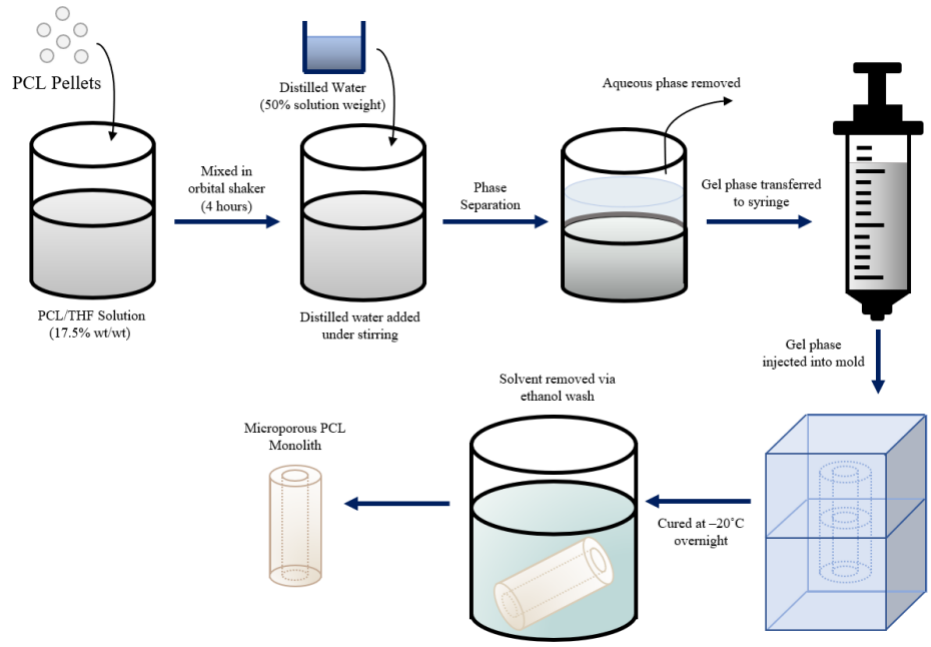

Figure 10. Diagram illustrating the phase separation casting technique employed for manufacturing PCL scaffolds.

2.3 Statistical Methods

The statistical analysis involved a one-factor analysis of variance (ANOVA) with subsampling, accounting for unequal variances. Kaleida Graph software 4.03 (Synergy Software, Reading, PA, USA) was employed for these analyses to assess whether the application of alginate had any significant impact on the mechanical and biological functionalities of PCL. In all instances of statistical testing, a significance level of $p < 0.05$ was adopted, indicating a statistically meaningful comparison.

Chapter 3

Experiments and Results

3.1 CAD model Development

To assess and demonstrate the implantation of the interlocking nail system and scaffold, a prototype rabbit tibia model was developed and printed. Initially, a publicly available CAD file of a rabbit tibia model served as the foundation.(Wong et al.; *Miguel Castro Ramos | GrabCAD*) Pre-existing channels for the nail and screws, along with a 20mm segmental defect, were integrated into the model before printing using Model V2 resin.

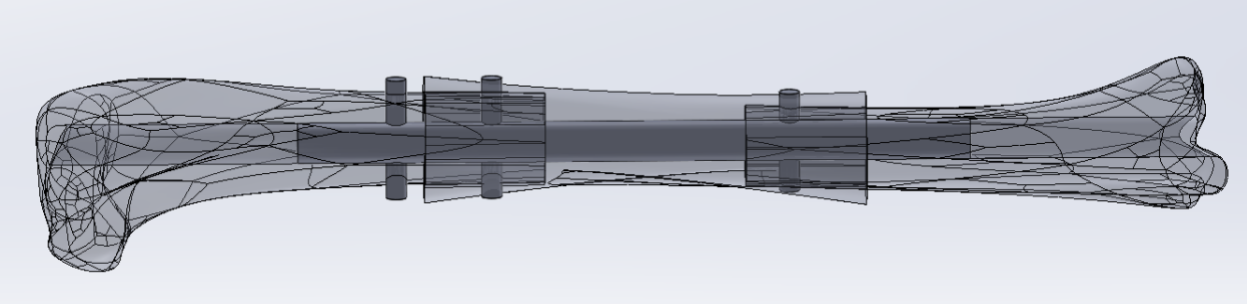

Figure 11. 3D demonstration model for bone tibia wireframe view.

3.2 Sample CAD design.

In this study, the goal was to identify a biodegradable material possessing sufficient strength for weight-bearing purposes and an appropriate compressive modulus to prevent stress shielding. The selected material for casting the scaffold, nail, and screws was Poly(ε-caprolactone) (PCL), as utilized by Wong et al. (Wong et al.), owing to its biodegradable nature and mechanical properties resembling those of bone. The casting process closely followed the procedures outlined by Wong et al..(Wong et al.) To enhance cell attachment and viability, the PCL bone

scaffold underwent a coating process with alginate, resulting in the creation of PCL-Alg. The subsequent sections detail the preparation methods for both PCL and PCL-Alg structures.

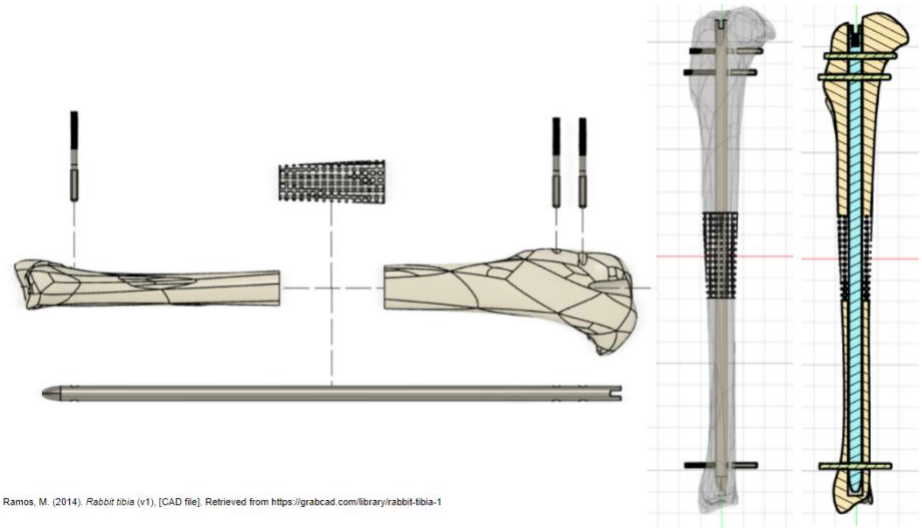

Figure 12**.** Diagram illustrating the designed components (bone scaffold, interlock nail, screw) for repairing a long bone defect using a tibia model in this study.

3.3. Design Specification of Interlocking Nail System

3.3.1. Design of Intramedullary Nail and Screws

Interlocking nail systems have seen advancements for large animals like cows, sheep, and dogs, but few cater to smaller animals like rabbits, specifically the rabbit tibia.(LeCronier et al.; Endo et al.) Existing systems predominantly use intramedullary nails and locking screws made of stainless steel or titanium alloy. (Endo et al.; LeCronier et al.; Khandaker et al.) Notably, none of the current solutions for rabbit tibia incorporate bioabsorbable materials or integrate an interlocked nail with a scaffold for treating segmental bone defects. Furthermore, the method of implantation lacks standardization across studies, with some inserting each end of the nail

through a central bone defect, while others make an incision below the knee and insert the nail through the proximal head of the tibia.

The development of the interlocking nail system for the rabbit tibia focused on three key design considerations: weight-bearing ability, biodegradability, and ease of implantation. These factors influenced the design of the interlock nail and screws, material selection, and the choice of production method. (Khandaker et al.)

Dimensions for the interlock nail and screws were initially based on the average measurements of rabbit tibias, following a study by Bakici et al..(Bakici et al.; Khandaker et al.) The average tibial length, internal tibial diaphysis diameter, and tibial proximal width were considered. The interlock nail was designed to be 3.5 mm in diameter with a length of 110 mm to fit within the medullary cavity. A "bullet nose" geometry aided implantation into the cavity, while the proximal end featured a hole for attachment to the targeting jig. Two 1.5 mm centrally smooth screws were designed for locking the proximal end, while only one screw was used for the distal end to avoid fractures in thinner tibial sections.(LeCronier et al.; Khandaker et al.) Solid Work software was employed for modeling the rabbit tibia based on these dimensions, with a 20 mm bone cut from the model to create the 3D model of the bone scaffold as shown in Figure13.

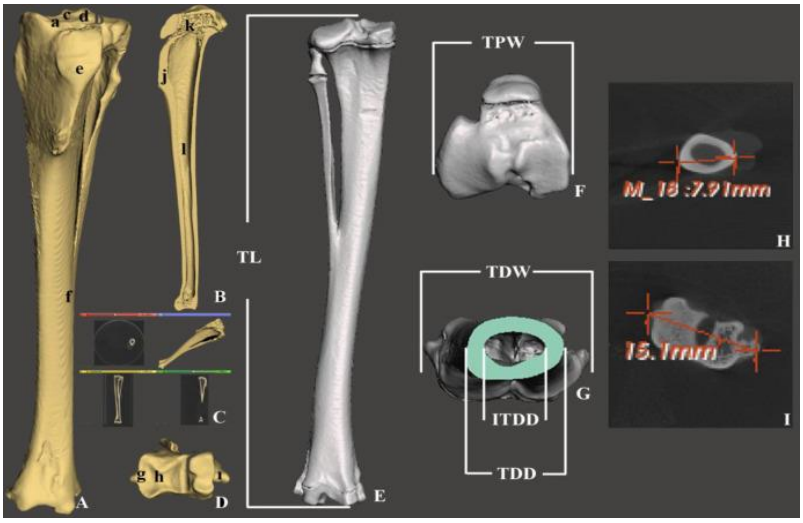

Figure 13. 3D reconstruction of Rabbit Tibia with example dimensions.

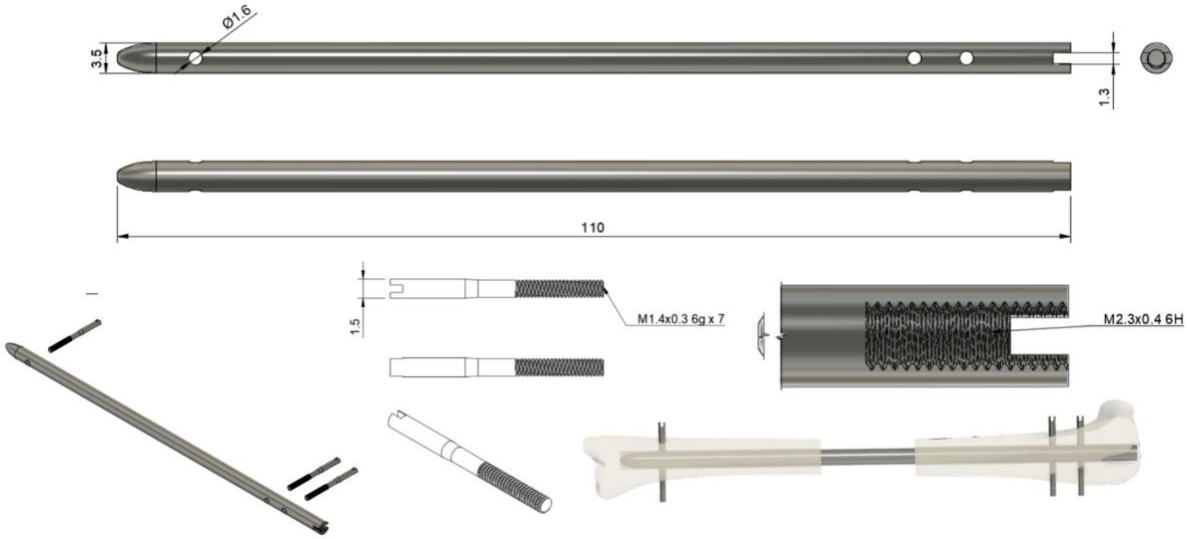

Figure 14 Drawings depicting the model of the intramedullary nail and interlocking screw.

3.3.2. Interlocking Nail System Material and Production

Various production methods were evaluated for the intramedullary nail and interlocking screws, including 3D printing, CNC machining, and casting. The selected method aligned with the phase separation technique used for casting the scaffold. Resin-printed masterpieces made of photopolymer resin were chosen to create negative molds due to the precision offered by this material and printing method, as demonstrated in Figure 15**.** Silicone was used to create a two-part mold with embedded rods and screws to shape the cast parts, as illustrated in the accompanying Figure 16.

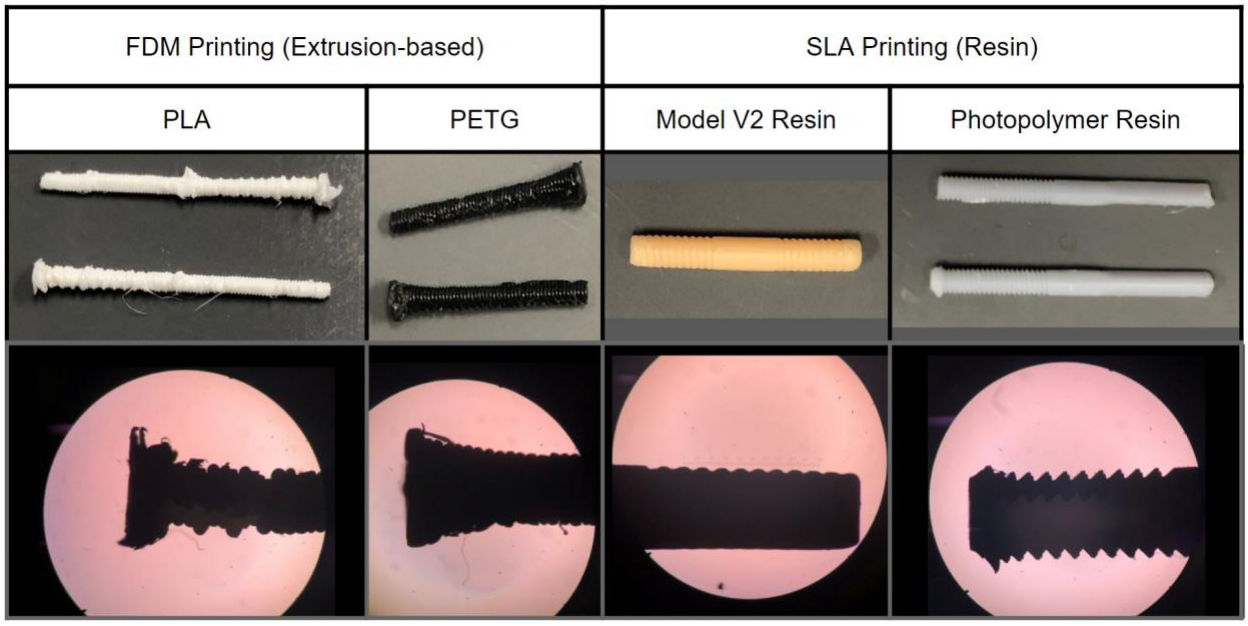

Figure 15. Comparison of screw thread precision for different 3D printing methods and materials.

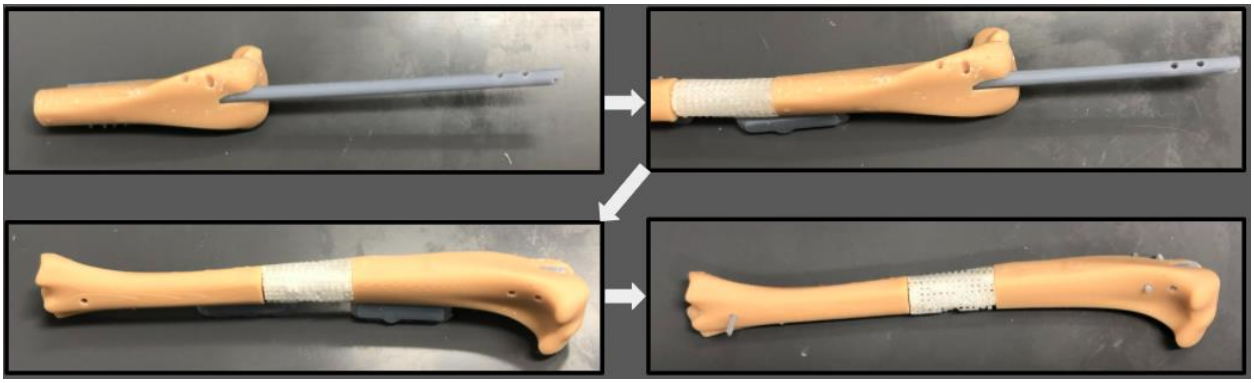

Figure 16. Demonstration of interlocking nail system and scaffold implantation steps.

For this project, selecting a biodegradable material with suitable strength for weight-bearing and an adequate compressive modulus to avoid stress shielding was crucial. (Khandaker et al.)After evaluating various materials, a magnesium-PCL composite, as utilized by Wong et al., was chosen for casting the nail and screws. This material was preferred for its biodegradability and similar mechanical properties to bone.(Wong et al.; Khandaker et al.) The casting process followed specific steps, including the addition of magnesium microparticles at a ratio of 40% wt/wt. with PCL pellets into the initial solution, following the procedure outlined on the designated page.

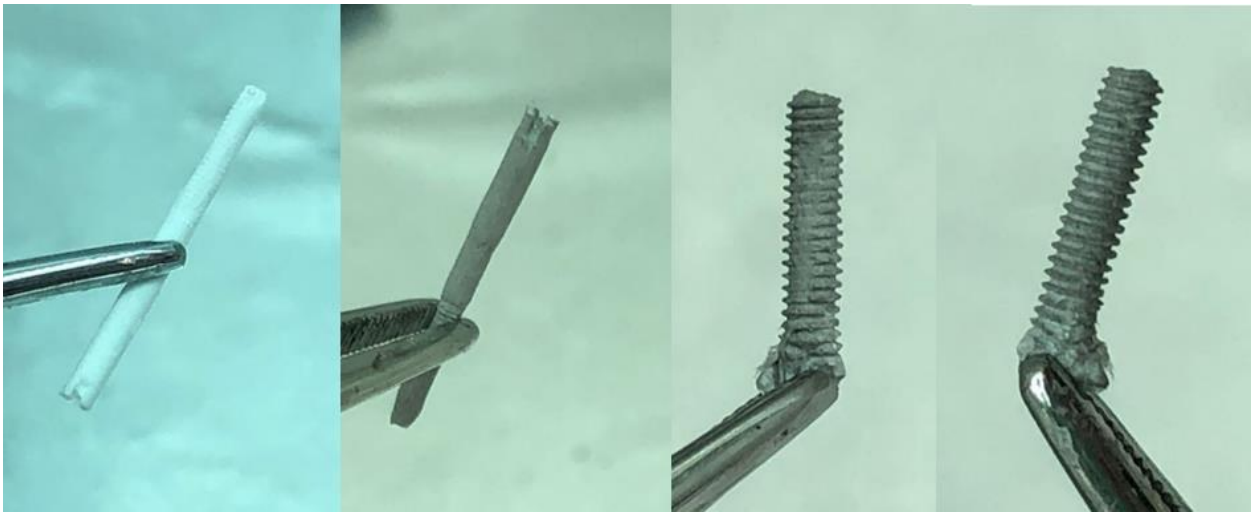

Figure 17. PCL and PCL-Mg screws cast using phase separation technique.

The phase separation technique proved effective in casting the PCL-Mg intramedullary nail and interlocking screws. However, issues with sealing the two-part molds and injecting the gel phase evenly throughout the mold resulted in hollow sections within the cast, diminishing the mechanical stability of the pieces and causing deformation further from the injection point. Nevertheless, the precision was maintained - PCL-Mg screws displayed visible threading, as shown in Figure 17, and the fixator pin could be securely screwed into the proximal end of the nail with an excellent fit, as depicted in Figure 13.

Table 1**.** Comparative Analysis of Interlocking Nail System Materials

	PCL	Mg-PCL	PLA	PVA	Model V2 Resin	Photopolymer Resin	Titanium
Bioabsorbable	✔	✔	✔	✔	✗	✗	✗
Water Soluble	✗	✗	✔	✔	✗	✗	✗
Melting Point (°C)	60-65	60-65	170-180	200-230	240-250	~150	~1650
Compressive Modulus (mPa)	200-250	260-360	80-100	< 1			

3.4. Design Specification of Targeted Jig

A custom targeting jig was meticulously designed to facilitate the minimally invasive implantation of the interlocking nail system, requiring little to no visual assistance during surgery. This innovative design comprised several key components: a fixator piece securely fastened to the end of the nail at a precise angle using a 2 mm screw, a handle affixed to the fixator for manual insertion of the nail into the medullary cavity, and an alignment arm featuring proximal and distal screw channels to ensure accurate placement of screws into the pre-drilled holes of the nail. The intricate parts of the jig were meticulously modeled and assembled utilizing SolidWorks 3D CAD design software, as depicted in Figure 18. The handle and arm pieces underwent FDM (extrusion) printing using PETG material, while the fixator and channels were crafted through SLA printing with clear photopolymer resin.

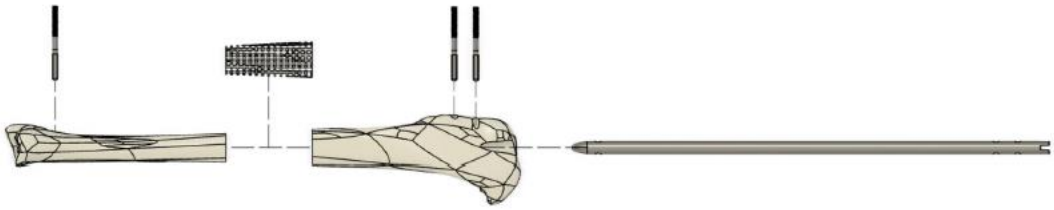

Figure 18. prototype used to demonstrate implantation system. (bone scaffold, interlock nail, screw)

3.4.1 Targeting Jig Design, Material and Production

The targeting jig plays a crucial role in ensuring precise alignment during the implantation of the interlocking nail system. It comprises a fixator, handle, arm attachment, and channels, all working in unison to maintain the correct alignment of screws during the implantation process. Designed for minimally invasive implantation with minimal visual assistance, the fixator piece locks to the end of the nail at a specific angle using a 2 mm screw. A handle is attached to the fixator for manual insertion of the nail into the medullary cavity, and an alignment arm with proximal and distal screw channels ensures the proper placement of screws into the pre-drilled holes of the nail. The Solid Works 3D CAD design software was employed to model and assemble the jig parts, as depicted in Figures 19 and 20.

To facilitate minimally invasive implantation of the interlocking nail system, a custom targeting jig was meticulously designed, aiming for a procedure with minimal visual assistance during surgery. This innovative design comprised a fixator piece that securely locked to the end of the nail at a specific angle, achieved through a 2 mm screw. A handle, seamlessly attached to the

fixator, facilitated the manual insertion of the nail into the medullary cavity. An alignment arm, featuring proximal and distal screw channels, ensured the precise placement of screws into the pre-drilled holes of the nail. The handle and arm pieces were manufactured through Fused Deposition Modeling (FDM) using PETG, while the fixator and channels were realized through Stereolithography (SLA) printing, employing clear photopolymer resin. Figures 19 and 20 vividly showcase the modeled and assembled components of the targeting jig.

Figure 19. Assembled targeting jig design with intramedullary nail.

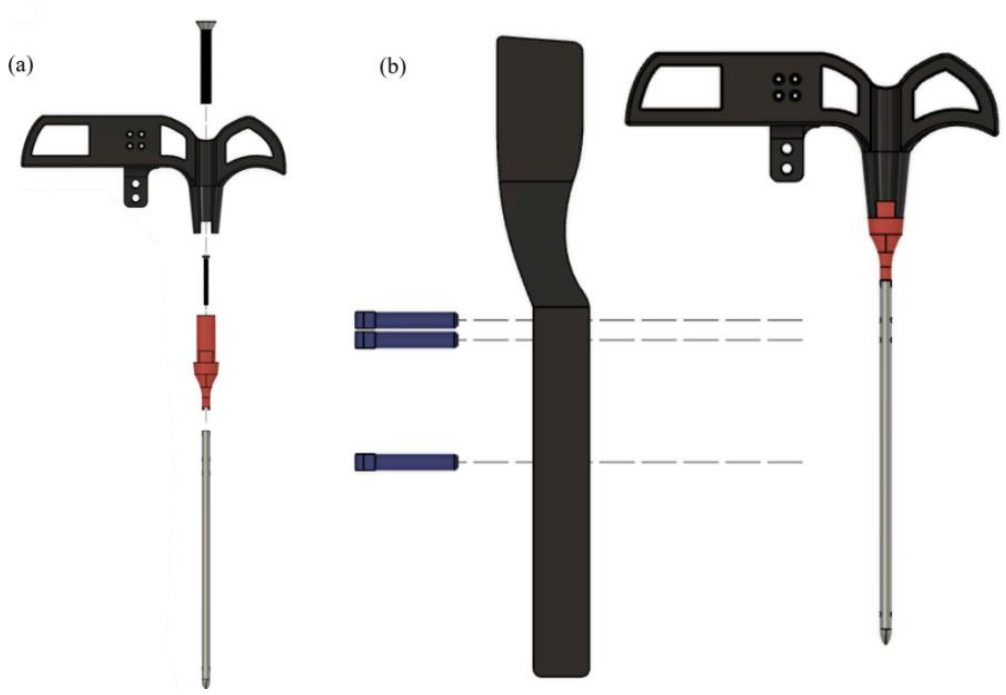

Figure 20. Exploded views of targeting jig design

3.4.2 Fabrication of Bone Scaffold, and Interlocking Nails and Screws

The utilization of the phase-separation technique in the casting method proved successful in creating microporous scaffolds composed of PCL. (Grandi et al.) Although some minor post-processing was required to address defects in the silicone molds, the overall outcome demonstrated the effectiveness of this method in producing bone scaffolds, interlocking nails, and screws, as depicted in Figure 20.

(a) Produced PCL bone scaffolds.

(b) Intermodular screw and interlock nails using the phase separation casting method. (Grandi et al.)

(a)

(b)

Figure 21. (**a**) Produced PCL bone scaffolds (**b**) intermodular screw and interlock nails using the phase separation casting method.

3.5. Experiments

3.5.1 Surface Characterization

The SEM surface images and pore distribution analysis of both PCL and PCL-Alg scaffolds are depicted in Figure 22. Comparing the two, fewer surface pores were evident on the PCL scaffold

MATLAB image processing analysis, it was determined that approximately 11% of the surface area of the PCL scaffold image contained pores. However, due to the infiltration of alginate into the pores of the PCL-Alg scaffold, accurate calculation of the total surface pore area from the

SEM image was hindered. Pore size parameters varied across different locations, with measured pore diameters ranging from 0.05 µm to 18 µm.

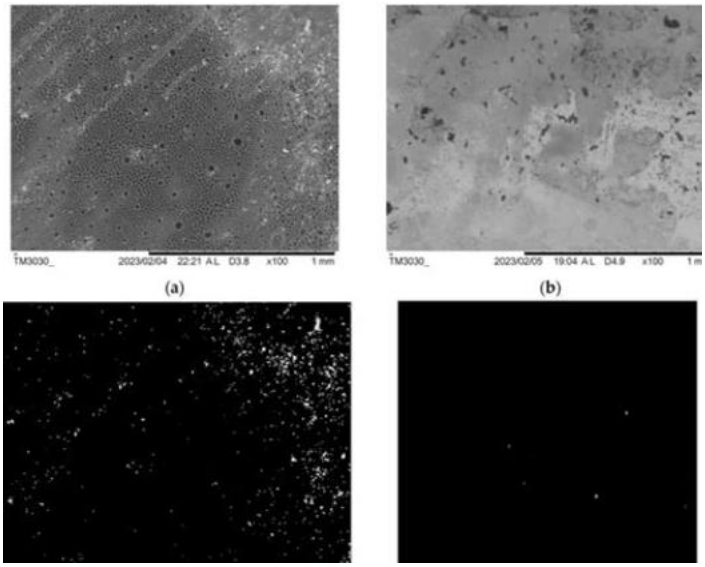

Figure 22. illustrates SEM images capturing the top surface of both (a) PCL and (b) PCL-Alg scaffolds. MATLAB binary images are provided to showcase the representation of white pixels as holes and black pixels as solid areas from the SEM images of (c) PCL and (d) PCL-Alg.

PCL Bone Scaffolds

The design and fabrication of the scaffold posed challenges, leading to a shift away from the extrusion-based 3D printing method. The focus shifted towards the electrospun nanofiber method and the phase separation casting method for scaffold creation. Ongoing studies aim to identify potential improvements in scaffold quality, and additional testing will explore ways to enhance the efficiency of scaffold production for biomechanical testing.

Interlocking Nail System

Enhancing the mechanical stability of the small-scale intramedullary nail and screws is a priority. This may involve the creation of new silicone molds with fewer defects or finding a more reliable production method that ensures increased strength. While the targeting jig is functional, there is room for improvement, possibly through channel size adjustments or employing a different tool to enhance control during screw implantation. Once a robust intramedullary nail and interlocking screws are produced, and the targeting jig is refined, the entire system will undergo testing through implantation into cadaver rabbit tibiae.

3.6 Examination Outcomes

3.6.1 Surface Morphology Analysis of Bone Scaffold

For the examination of bone scaffold surface morphology, the top surfaces of both PCL and PCL-Alg scaffolds were observed at arbitrary locations utilizing a Hitachi TM 3000 Scanning Electron Microscope (Hitachi High-Technologies Corporation, Nake, Japan). These observations were crucial for a qualitative comparison of the scaffold.

To quantify the total pore area, an image-processing algorithm in MATLAB was employed. Additionally, the pore size measurements were conducted using the USA National Institute of Health ImageJ software (Version 1.53). These sophisticated analyses provided a detailed understanding of the structural characteristics of the bone scaffolds, contributing valuable insights to the overall assessment.

3.6.2 Mechanical Testing and Analysis

Following the design and fabrication of the various scaffolds, a mechanical assessment was conducted to evaluate their hardness and mechanical characteristics. The assessment involved subjecting the scaffolds to a compression test, compressing them by two millimeters. Additionally, a stress and strain analysis were conducted to gauge the scaffolds' capacity to withstand external forces.

To perform the compression test, a Test Resources Inc tensile/compression mechanical test system (depicted in Figure 23) was employed. Silicone molds with dimensions of 10 mm diameter and 8 mm height were utilized to cast the scaffolds, following the procedure outlined in **Section 2.3.** Each set of samples was mounted between the holders in the test system, and compression was applied to the scaffold height at a rate of 0.05 mm/sec during the unconfined compression test.

Figure 23. Compression test of a round PCL sample (diameter 9.8 mm and 7.8 mm height) in a Test Resource Universal Testing Machine

The load borne by the scaffold and the corresponding displacement were directly recorded using the testing machine software and then exported to Microsoft Excel. Subsequently, stress (load/cross-sectional area) and strain (displacement/initial height) curves were generated from these data. The slopes of these curves were analyzed to assess differences in compressive strength and modulus among the samples.

stiffness (KN/m)
105.94
105.29
90.89
100.7066667
8.507692597
3.804755796

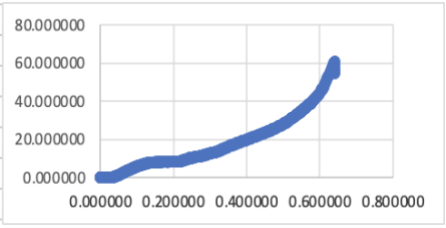

Figure 24. Stress-Strain curve or extrusion-based 3D PCL scaffold.

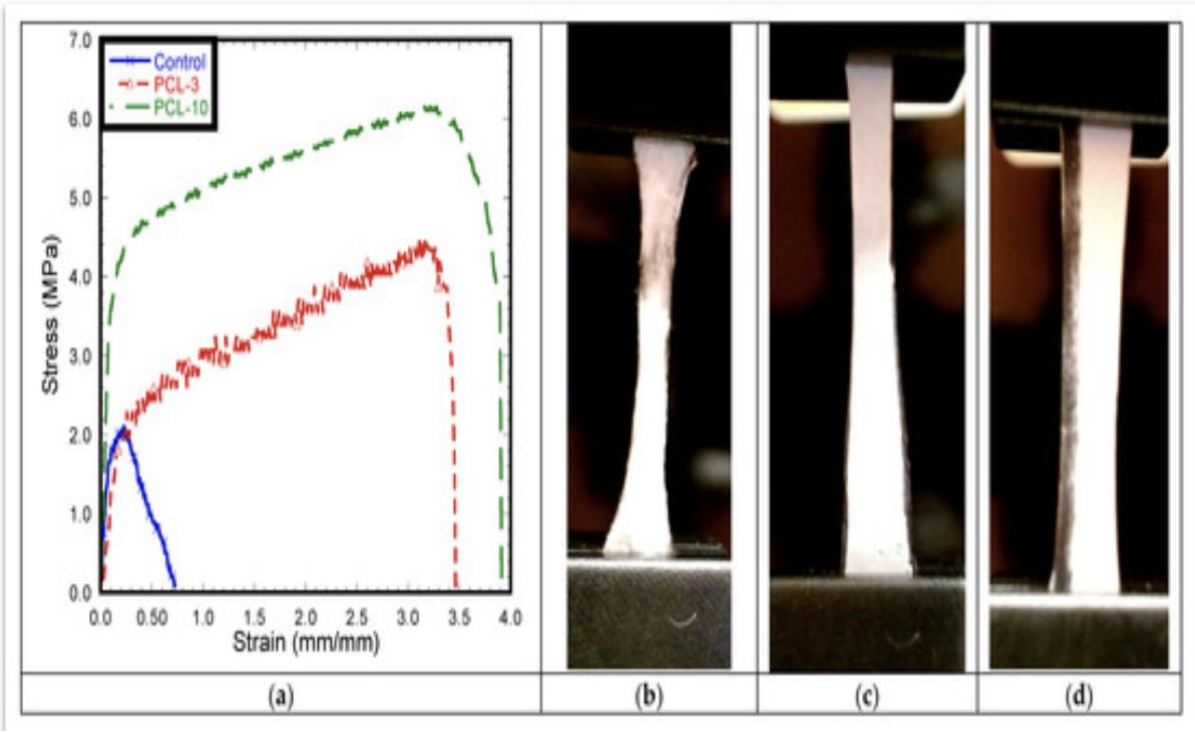

Figure 25. Stress-Strain curve of PCL nanofiber.

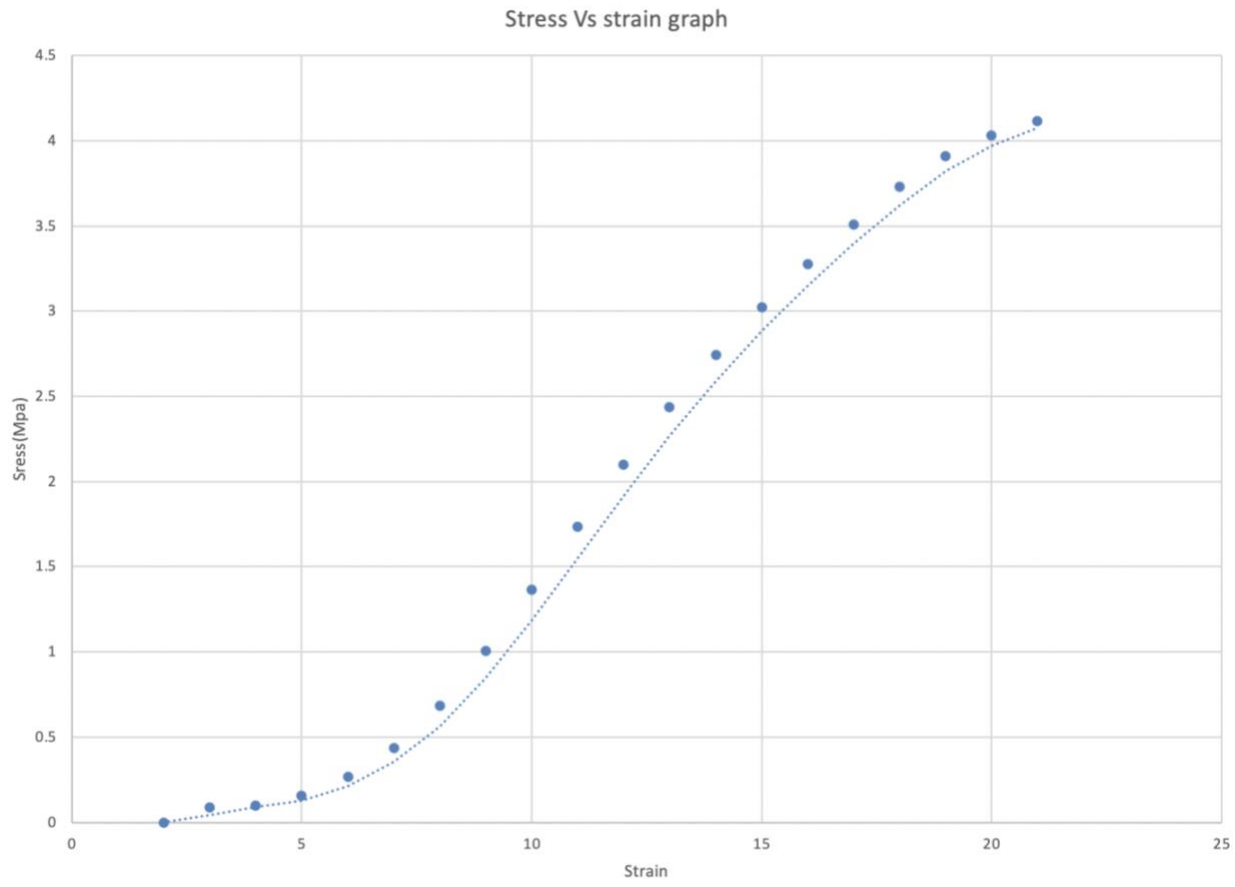

Figure 26. Stress-Strain curve of casted PCL scaffold.

To evaluate the compression performance of each scaffold, the elastic modulus and maximum stress were determined. The maximum stress, representing the point of peak stress, was derived from the stress-strain curve illustrated in Figure 24, 25 and 26. The elastic modulus was computed from the slope of the stress-strain curve, considering the data points until the initial occurrence of sudden displacement. The average of the results obtained from three samples was considered as the final test outcome.

3.6.3. Water Absorption and Degradation Assessment

Water absorption characteristics of both PCL and PCL-Alg were evaluated through immersion in deionized water for one hour. The initial weight (W0) of three samples from each scaffold group was recorded. Following the immersion period, the weight of the scaffolds (Wt) was measured. The percentage of water absorption was calculated using the formula: $(Wt - W0) \times 100\%/W0$.

Additionally, a degradation test was carried out with six additional samples (n = 3/group). The same six types of samples used in the cell viability assay were utilized for this degradation test. Each sample group consisted of four test samples, and the results were averaged. The change in mass after seven days of immersion in PBS was analyzed, and the results are presented in Figure. These samples underwent submersion in PBS to assess the percentage change in mass after 7 days. This comprehensive analysis provides valuable insights into the water absorption and degradation properties of the scaffolds, contributing to a thorough understanding of their performance characteristics.

To evaluate the degradation characteristics, a comprehensive degradation test was performed on the same six sample types utilized in the cell viability assay. Each sample group comprised four test samples, and the results were averaged analysis. Submersion in PBS was employed to assess the change in mass over a 7-day period, and the outcomes are presented in Figure 28.

The test results revealed variations among the samples, with some exhibiting a positive change in mass due to PBS absorption, while others displayed a decrease attributed to the degradation of the hydrogel coating. It's essential to note that the test faced certain challenges, particularly concerning the method employed for drying the samples before weighing. This may have

introduced some inaccuracies into the results. The use of an alternative drying method or an extended test duration could potentially enhance the precision of future degradation assessments.

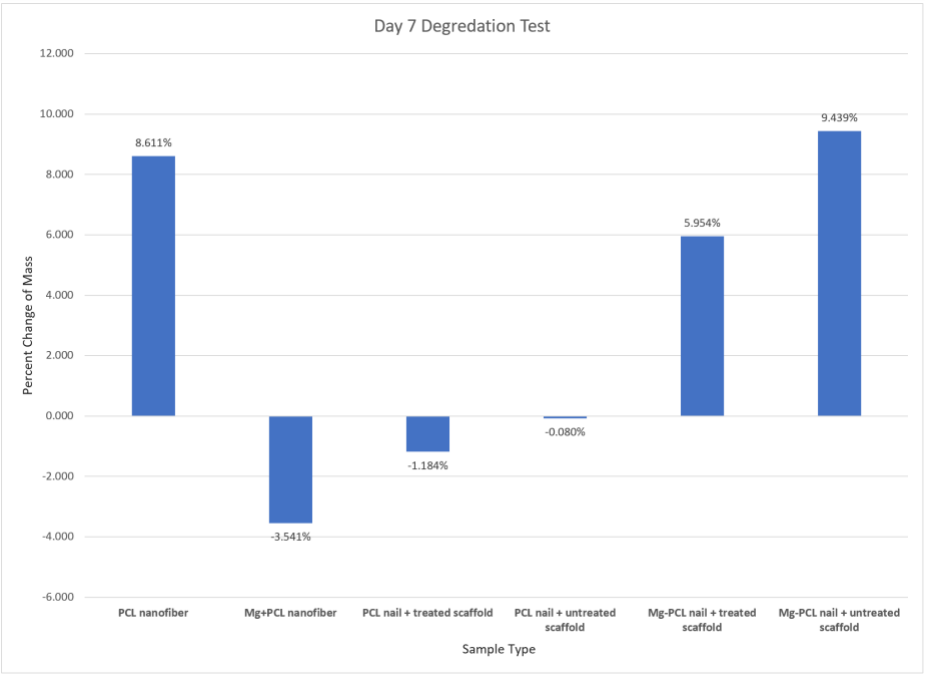

Figure 27. Degradation Test Results

3.7 Targeting Jig Efficacy Assessment

3.7.1 Invitro Validation

The targeting jig components were crafted and assembled, as depicted in Figure 11. Employing biocompatible PLA material, the handle and arm sections were Formlabs FDM (extrusion) printed, while the fixator and channels were produced using Formlabs BioMed Amber Resins. Slight adjustments in the modeling of the screw holes ensured proper joint clearance. The targeting jig was effectively employed in the ex vivo demonstration, showcasing the implantation of a resin-printed nail and screws into a transparent 3D-printed rabbit tibia model. The rabbit tibia model, representing a 20 mm cut along the tibia's center, facilitated the installation of nails

and screws according to the outlined procedure in **Section 2.6.** This validation process aimed to verify the precision of the fabricated components before advancing to the cadaveric study.

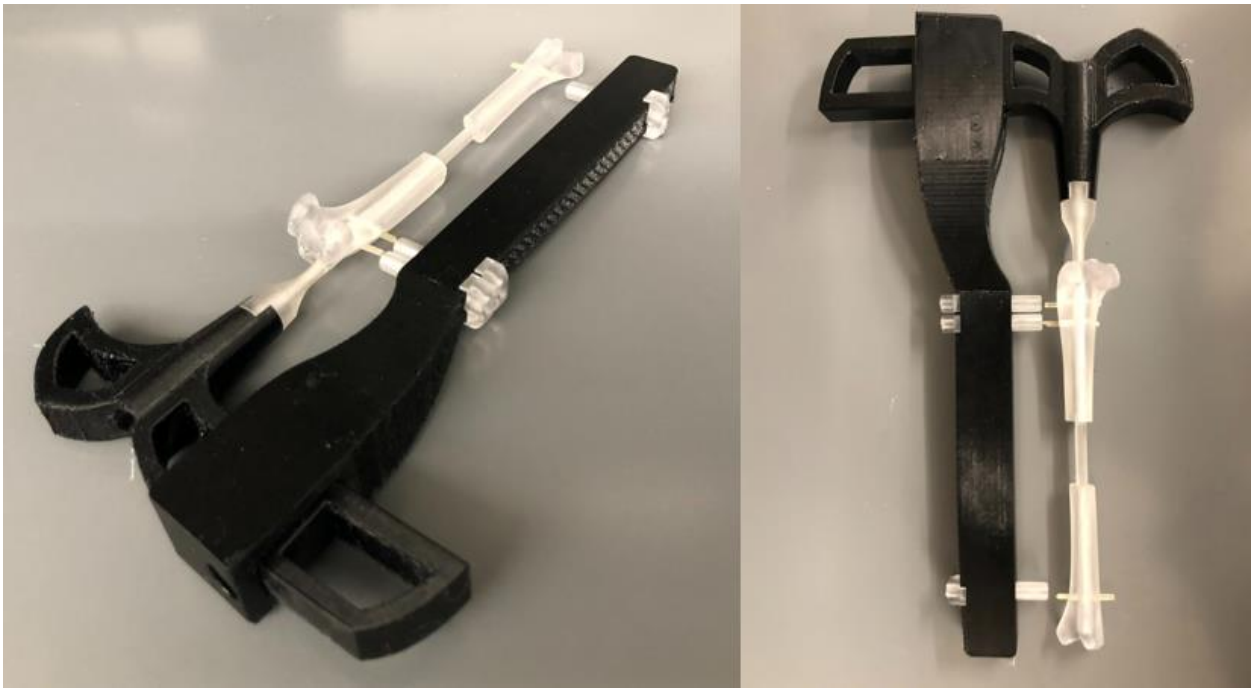

Figure 28. (a) The 3D printed targeting jig. (b) Efficacy tests of the fabricated delivery jigs using a 3D-printed rabbit tibia model, demonstrating the jig's capability to install an intramedullary nail and screws into a 20 mm-long rabbit tibia defect

3.7.2 Cadaveric Assessment and Proposed Advancements

In our thorough cadaveric exploration, we proficiently addressed a 20 mm long bone defect through the application of the PCL bone scaffold, complemented by interlocking nails and screws in both legs of a rabbit. This process adhered to the specified protocol outlined in Section 2.5. The stepwise implementation for one leg is visually depicted in Figure 29 a–d, delineating the successive stages of scaffold, nail, and screw integration. Furthermore, Figure 29 e presents the holistic installation of the scaffold, nail, and screws, featuring an additional screw firmly

secured through the scaffold and nail, emphasizing the drill ability of the PCL scaffold and nails. (Grandi et al.)

Furthermore, Figure 28 presents the holistic installation of the scaffold, nail, and screws, featuring an additional screw firmly secured through the scaffold and nail, emphasizing the drill ability of the PCL scaffold and nails. (Grandi et al.)

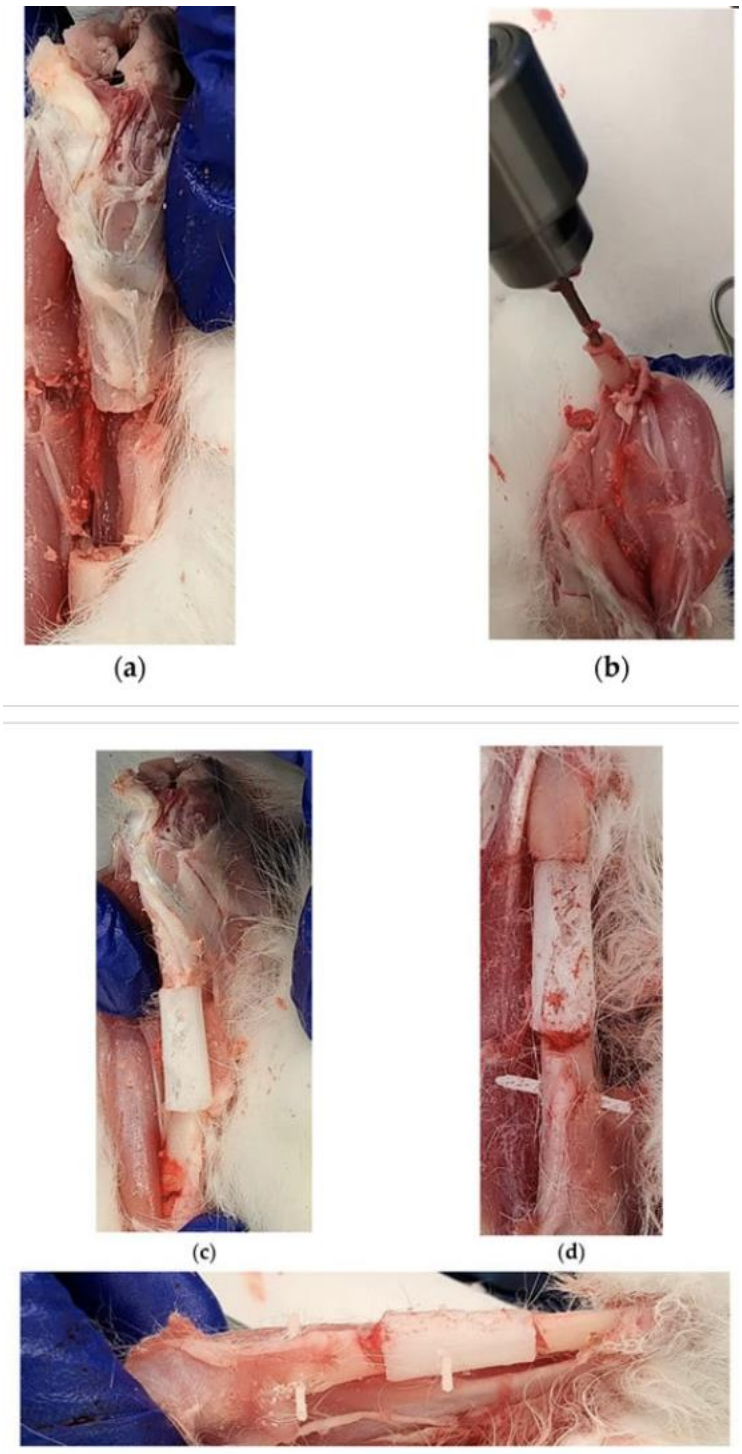

Figure 29. First leg: (a) Creation of a 20 mm long bone defect using an orthopedic oscillating bone saw; (b) Formation of intramedullary holes for the nail; (c) Scaffold installation with

interlocking nails; and (d) Secure fastening of nails to the tibia bone using a screw. Second leg: (e) Secure fastening of the scaffold with a nail through a screw in an installed interlocking nail system within a long bone defect model.

Moreover, the existing challenges associated with healing a segmental bone defect are formidable, lengthy, and often entail considerable discomfort for both surgeons and patients. Our proposed solution, incorporating a bioabsorbable interlocking nail system and scaffold, aims to address numerous shortcomings inherent in current methods. The anticipated improvements encompass:

- Enhanced stability attributed to the interlocking nail.
- Reduced recovery duration facilitated by the scaffold.
- Load-bearing support during the recovery process, courtesy of the scaffold.
- Elimination of the necessity for additional surgeries to remove implants due to their bioabsorbable nature.

Chapter 4

Discussion

4.1. Bone Reconstruction: From Design to Practical Implementation

The American Academy of Orthopedic Surgeons reports a staggering 6.3 million fractures annually in the United States, with bone grafting procedures exceeding 500,000 and costing approximately $2.5 billion. This has propelled the search for bone-grafting alternatives, driven by issues such as limited availability, donor site pain, prolonged surgery times, and heightened infection risks. Of particular concern are critical size bone defects, causing significant clinical and socioeconomic challenges, resulting in extended hospitalizations and repeated reoperations, detrimentally affecting patients' quality of life.

In response to these challenges, our study successfully conceptualized and prototyped a 3.2 mm diameter interlock nail and a 1.0 mm diameter fixation screw using an established polymer casting technique. A custom silicon mold facilitated the production of a porous PCL bone scaffold, further enhanced by coating with alginate to yield the PCL-Alg scaffolds. (Grandi et al.)Water absorption, degradation, and mechanical assessments showcased the suitability of both PCL scaffolds for water absorption and early weight-bearing. The scaffold's porosity allowed alginate hydrogel infiltration, enhancing water absorption and biodegradation profiles. Additionally, cell viability results revealed alginate's positive influence on PCL scaffold cell viability.

The innovation extended to the creation of a targeting jig, aiding precise alignment and placement of the interlock nail and fixation. In vitro efficacy tests, involving a 3D-printed rabbit tibia and cadaver, underscored the jig's potential for future in vivo studies. The Alamar blue

assay demonstrated a linear correlation between reduction and cell number, providing a comprehensive understanding of cell viability on various samples over different durations.

Mechanical characteristics assessment indicated scaffold compressive strength (9.51 ± 0.24 MPa) closely aligning with human cancellous bone (1.5-12 MPa). Nevertheless, improvements in mechanical stability for the interlock nail and screw fixation were identified as key areas for refinement.

Addressing the challenge of interlocking nail system development for rabbit tibiae, we sought higher mechanical stability for better weight-bearing. The phase separation method succeeded in producing a robust scaffold but faced challenges in creating smaller interlock nail and screw components, resulting in larger-than-expected hollow sections.

Our study, while focused on surface pore analysis, lays the groundwork for future porosity and interconnectivity studies. Histological analysis, essential for evaluating cell infiltration, remains a key avenue for exploration in future in vivo studies.

Despite designing the bone scaffold for an eight-week-old rabbit, successful cadaveric studies with different-aged rabbits suggested potential patient-specific modeling through microcomputed tomography. Future in vivo studies aim to evaluate mechanical stability through three-point bend and torsion tests post-implantation

4.2. New Implant Design, Evaluation, and Refinements

Development of the scaffold posed significant challenges, prompting the exploration of alternative methods. Initial attempts using the extrusion-based 3D printing method proved impractical for scaffolds exceeding 10 mm in length.

For the interlocking nail system, a major hurdle was the need for a compact size tailored to fit the dimensions of a rabbit tibia. Striking a balance between achieving higher mechanical stability for weight-bearing purposes and utilizing biodegradable materials posed difficulties. Precision in production, especially concerning intricate details, proved challenging due to the limitations of the less precise production methods associated with PCL when compared to metals.

While the phase separation method demonstrated great success in producing scaffolds, adapting it for the smaller, thinner components of the intramedullary nail and screws presented challenges during the injection process. This resulted in pieces with larger hollow sections than initially desired. Ongoing efforts are directed towards overcoming these challenges to enhance the precision and effectiveness of the interlocking nail system design.

4.3. Evaluation of Targeting Jig

The effectiveness of our designed targeting jig underwent rigorous testing, employing a 3D-printed rabbit tibia model and cadaveric experiments with rabbit specimens. The rabbit tibia model adhered to the dimensions outlined by Bakici et al. (Bakici et al.)A euthanized six-week-old female New Zealand white Rabbit (NWR), housed at the University of Oklahoma Health Science Center (OUHSC) animal care facility, was utilized for the cadaveric tests, following the methodology described by Huang et al.

Utilizing an orthopedic oscillating bone saw, a 20 mm defect (matching scaffold length) was created in the rabbit tibia, situated below the fusion point of the fibula and tibia. This defect, representing 20% of the tibia's length, aligns with the critical-sized defect criteria. (Laurencin et al.)Prior to tibia insertion, a sequence of drill bits (1 mm, 2 mm, 3 mm, and 3.8 mm) established a 3.8 mm hole along the medullary cavity, encompassing the cut end of the tibia. This drilling

resulted in a through hole at the proximal end and a blind-ended hole at the distal end, matching the length of the interlocking nail.

Insertion of the bone scaffold into the defect followed, with the nail subsequently introduced into the medullary cavity through the scaffold, guided by the targeting jig. Side holes were drilled to fasten the interlocking nails with the bone, facilitated by the targeting jig's side-hole alignment guide fixture. This fixture ensured the coaxial alignment of screws with the central axis of the bone, ensuring precise alignment with the pre-existing hole in the nail. The same procedure was replicated on the 3D-printed in vitro rabbit tibia model to assess the targeting jig's effectiveness.

Chapter 5

Conclusion and future work

In summary, the reconstruction of long-bone segmental defects is a formidable orthopedic challenge. Current methods are arduous, prolonged, and painful. Our proposed solution, featuring a bioabsorbable interlocking nail system and scaffold, addresses these challenges head-on. The project combines a unique PCL porous scaffold with or without alginate hydrogel and an interlocking nail system for small animal models, promising advancements in critical-size bone defect repair. Our findings highlight structural validity but also provide opportunities for optimization, ensuring superior biomechanical properties, immediate postoperative weight-bearing, and robust histological and structural bone tissue repair. The project's successful clinical translation will offer substantial benefits, marking a significant leap forward in orthopedic reconstructive solutions. A wide range of approaches and techniques, from modeling and design to literature analysis, have been employed and learnt. This year, we'll employ each of these methods to enhance our design and prototype, as well as to build and produce a better rabbit scaffolding and connecting system utilizing a five-dimensional CNC machine. The current methods for correcting a segmental bone deficiency are challenging, labor-intensive, and painful for the patient and the surgeon. Using a framework and a bioabsorbable interlocking nail system, this technology would solve a lot of the issues with current systems. The nail that interlocks provide stability. The scaffold shortens the recovery period. load bearing because of the scaffolding during the recuperation phase.

References

Bakici, CANER, et al. “Three Dimensional Modeling and Quantitative Analysis of Long Bone Parameters of Rabbit Using Micro-Computed Tomography.” *Iranian Journal of Veterinary Research*, vol. 22, no. 2, 2021, p. 140.

Capacchione, Clotilde, et al. “Poly (Ethylene Glycol)/β-Cyclodextrin Pseudorotaxane Complexes as Sustainable Dispersing and Retarding Materials in a Cement-Based Mortar.” *ACS Omega*, vol. 6, no. 18, 2021, pp. 12250–60.

Coombes, AGA, et al. “Precipitation Casting of Polycaprolactone for Applications in Tissue Engineering and Drug Delivery.” *Biomaterials*, vol. 25, no. 2, 2004, pp. 315–25.

Dang, Thi Thanh Le, et al. “Eco-Friendly Facile Synthesis of Co3O4–Pt Nanorods for Ethylene Detection towards Fruit Quality Monitoring.” *Sensors and Actuators A: Physical*, vol. 362, 2023, p. 114607, https://doi.org/10.1016/j.sna.2023.114607.

Endo, Kaoru, et al. “Interlocking Intramedullary Nail Method for the Treatment of Femoral and Tibial Fractures in Cats and Small Dogs.” *Journal of Veterinary Medical Science*, vol. 60, no. 1, 1998, pp. 119–22.

Fernandes, Marco Bernardo C., et al. “The Effect of Bone Allografts Combined with Bone Marrow Stromal Cells on the Healing of Segmental Bone Defects in a Sheep Model.” *BMC Veterinary Research*, vol. 10, 2014, pp. 1–12.

Ferreira, Nando, and Yashwant S. Tanwar. “Systematic Approach to the Management of Post-Traumatic Segmental Diaphyseal Long Bone Defects: Treatment Algorithm and Comprehensive Classification System.” *Strategies in Trauma and Limb Reconstruction*, vol. 15, no. 2, 2020, p. 106.

Fuchs, Julie R., et al. “Tissue Engineering: A 21st Century Solution to Surgical Reconstruction.” *The Annals of Thoracic Surgery*, vol. 72, no. 2, 2001, pp. 577–91.

Grandi, Claudio, et al. “Porous Alginate/Poly (ε-Caprolactone) Scaffolds: Preparation, Characterization and in Vitro Biological Activity.” *International Journal of Molecular Medicine*, vol. 27, no. 3, 2011, pp. 455–67.

Khandaker, Morshed, et al. “Evaluation of a Bioabsorbable Scaffold and Interlocked Nail System for Segmental Bone Defect.” *Journal of Functional Biomaterials*, vol. 14, no. 4, 4, Apr. 2023, p. 183. *www.mdpi.com*, https://doi.org/10.3390/jfb14040183.

Laurencin, Cato, et al. “Bone Graft Substitutes.” *Expert Review of Medical Devices*, vol. 3, no. 1, 2006, pp. 49–57.

LeCronier, David J., et al. “Development of an Interlocked Nail for Segmental Defects in the Rabbit Tibia.” *Proceedings of the Institution of Mechanical Engineers, Part H: Journal of Engineering in Medicine*, vol. 226, no. 4, 2012, pp. 330–36.

Mauffrey, Cyril, et al. “Management of Segmental Bone Defects.” *JAAOS-Journal of the American Academy of Orthopaedic Surgeons*, vol. 23, no. 3, 2015, pp. 143–53.

Miguel Castro Ramos | GrabCAD. https://grabcad.com/miguel.castro.ramos-1. Accessed 20 Mar. 2024.

Murry, Charles E., and Gordon Keller. “Differentiation of Embryonic Stem Cells to Clinically Relevant Populations: Lessons from Embryonic Development.” *Cell*, vol. 132, no. 4, 2008, pp. 661–80.

Sudhakar, C. K., et al. “Chapter 5 - Hydrogels—Promising Candidates for Tissue Engineering.” *Nanotechnology Applications for Tissue Engineering*, edited by Sabu Thomas et al., William Andrew Publishing, 2015, pp. 77–94, https://doi.org/10.1016/B978-0-323-32889-0.00005-4.

Vacanti, Charles A. “The History of Tissue Engineering.” *Journal of Cellular and Molecular Medicine*, 2006.

Wei, Qinghua, et al. “Modification, 3D Printing Process and Application of Sodium Alginate Based Hydrogels in Soft Tissue Engineering: A Review.” *International Journal of Biological Macromolecules*, vol. 232, 2023, p. 123450.

Wong, Hoi Man, et al. “Low-Modulus Mg/PCL Hybrid Bone Substitute for Osteoporotic Fracture Fixation.” *Biomaterials*, vol. 34, no. 29, 2013, pp. 7016–32.

Yang, Yunzhi Peter, et al. “Osteoinductive 3D Printed Scaffold Healed 5 Cm Segmental Bone Defects in the Ovine Metatarsus.” *Scientific Reports*, vol. 11, no. 1, 2021, p. 6704.